



# **FILM THICKNESS MEASUREMENT OF MECHANICAL SEAL BASED ON CASCADED ARTIFICIAL NEURAL NETWORK RECOGNITION MODEL**

Erqing Zhang, Pan Fu, Kesi Li, Xiaohui Li, Zhongrong Zhou  
School of Mechanical Engineering  
Southwest Jiaotong University, Er Round Road 111#  
Cheng Du, Sichuan 610031, China  
Emails: zrq@my.swjtu.edu.cn

---

*Submitted: Aug. 22, 2014*

*Accepted: Nov. 2, 2014*

*Published: Dec. 1, 2014*

---

*Abstract- Mechanical seal end faces are separated by a thin fluid film. The thickness of this film must be optimized so as to preventing the serious friction of two end faces and minimizing the fluid leakage. The micro scope condition monitoring of end face is of importance to ensure mechanical seals run normally. A method for measuring the film thickness of end faces and detecting the friction of end faces of mechanical seal has been presented in this paper. Eddy current sensors embedded in the stationary ring of mechanical seals are used to directly measure the thickness of the liquid-lubricated film. The Eddy current signal is decomposed by empirical mode decomposition into a series of intrinsic mode function. The information reflecting the film thickness is obtained by eliminating the false intrinsic mode function components. Acoustic emission sensor placed on the lateral of stationary ring is*

*used to detect the friction of end faces. In order to decrease the acoustic emission signal's noise, wavelet packet and kernel principal component analysis are used to extract the data features. Then cascaded decision is presented to improve the recognition rate of artificial neural network, by which the film thickness can be estimated accurately. With a set of tests, the results demonstrate that the method is effective. It can be widely used to take measurement of the film thickness in industrial field.*

**Index terms:** Mechanical Seal; Film Thickness; Eddy Current; Acoustic Emission; Empirical Mode Decomposition; Artificial Neural Network.

## I. INTRODUCTION

Mechanical seal is one of the most important parts for rotating machineries, such as pumps, compressors, etc. Mechanical seal is used to seal chamber while the shaft is rotating. It is widely applied in the field of nuclear energy, petroleum, chemical industry, coal chemical, pharmaceutical, environmental protection and so on. Statistics shows that about 95% of the rotating equipments containing chemical process adopt mechanical seal for preventing medium leakage between power input shaft and shell [1]. Compared to traditional contact mechanical seal, non-contact seal need much lower consumption, but have much longer life and higher reliability. While the hydrodynamic effect occurs when rotating ring rotates with shaft, a liquid-lubricated film is formed between end faces of mechanical seal. The thickness of the liquid-lubricated film is related to leakage. If it is not so thin, the leakage will increase. But if it is not so thick, the friction of end face will occur. This phenomenon either reduces the life or lower reliability of the mechanical seal. Sometimes the hydrodynamic effect might be not strong enough to form a stable liquid-lubricated film, especially when the mechanical seals starting or stopping. Severe contacts of end face can be a disaster to factories and workers. In order to avoid this, the running condition of the mechanical seals must be monitored.

Many scholars have devoted to the research of the fluid film measurement. In early time, the fluid film had been measured via the approach of capacitance and resistance by Astridge [2] and Cameron [3] et al. Later Etsion [4] have proved that eddy current method to be useful. However, all these approaches can't be used in industry because it requires modifying the structure of the equipment. In 2001, ultrasonic sensor had been used by Anderson [5], but in his way, only seal

face contact could be detected. Sometime later, an improved approach based on ultrasonic technique was presented by Reddyhoff [6] to estimate the film thickness. But, this method was still unsuited for production, because of its expensive cost. Then, acoustic emission (AE) technique had been attempted by Miettinen [7]. However, limited by the level of signal processing at that time, it was unable to separate useful signal from noise since AE sensor was too sensitive to noise.

The purpose of this research is to develop a approach for monitoring the fluid film of Mechanical seals based on two kind of signal in industry. In this work, eddy current and AE techniques are used at the same time, and non-contact seal is took as the research object. The eddy current sensors are used to make directly measurement. The AE sensor is used to make indirectly measurement. Under the guidance of direct measurement, a cascaded artificial neural network recognition model is built based on AE signals, by which the film thickness can be estimated.

## II. DIRECT MEASUREMENT

### a. Monitoring Experiments

#### a.i Apparatus

For non-contact seal, a thin fluid film makes stationary ring and rotating ring separated and keeping lubricated. Two steel rings are inlayed in the seal rings. They are grinded paralleling with the seal end faces. Three eddy current sensors are utilized to measure the distance between the two rings. They are put through a small hole drilled on the steel ring, as Figure 1 shows.

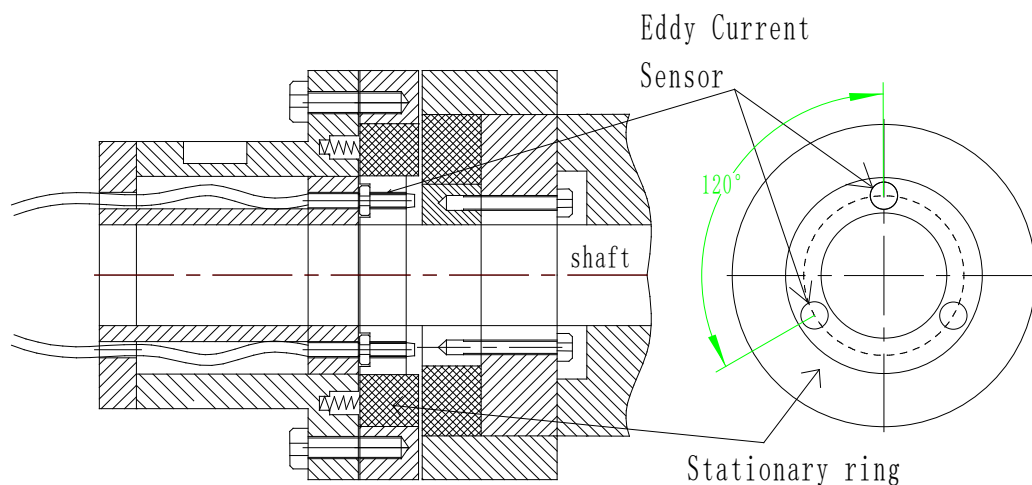


Figure 1. Eddy current test.

The experimental conditions are described in table 1

Table 1: Experimental conditions:

Conditions	Quantitative value
Spindle speed	0-1500r/s
Material of rotating ring	silicon carbide
Material of stationary ring	silicon carbide
Test medium	Deionized water
Temperature	20 ~ 80 °C
pressure	0.5MP, 2MP, 5MP, 10MPa

In Figure 1, the two seal rings are made of silicon carbide, and the two steel rings are made of SUS304. Eddy current sensor parameters are shown as following.

Type:KD2306; Range:0.5mm; Resolution:0.1um; Nonlinearity<1%; Frequency response:50KHz.

#### a.ii Experiment Data

With deionized water as sealing medium, two group experiments are designed under the condition of variable speed and pressure. The spindle speed is varied from 0 to 1500 r•min<sup>-1</sup>, and the water pressure is 0.5MPa, 2MPa, 5MPa, and 10MPa.

Limited by the processing level, the measurement surface is not strictly paralleling with the seal end faces. The eddy current signal amplitude have a great variation range when hand turning, which is shown in Figure 2. The curve maximum value is 3.6291(V), the minimum value is 2.9501(V). The peak-to-peak value is 0.679V(equivalent to 33.95um). This value is far thicker than the normal film thickness, so the original signal must be carried out filter processing.

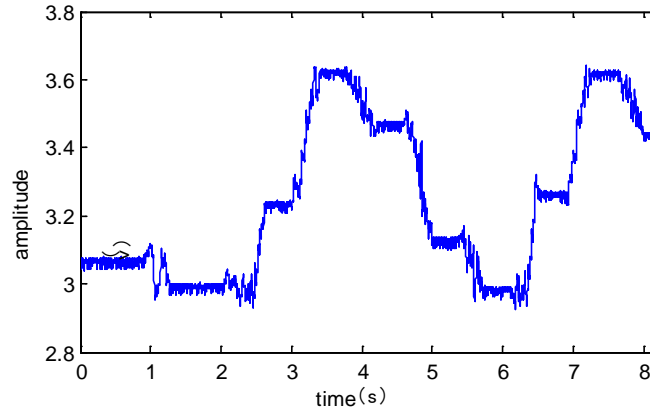


Figure 2. Curve of eddy current when hand turning.

The eddy current signal is obtained with constant pressure and variable speed, which is shown in Figure 3. Since the inlaid rings can't be kept absolutely parallel with the seal faces, sine wave can be obviously observed. The actual value of the film thickness can be picked up by the empirical mode decomposition (EMD) method.

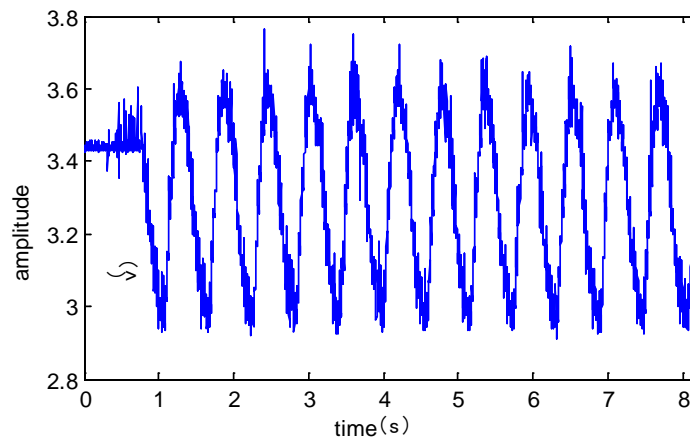


Figure 3. Curve of eddy current.

## b. Method

### b.i EMD

Traditional signal time-frequency analysis method is almost based on Fourier transform, which have many limitations of itself. In 1998, National Aeronautics and Space Administration(NASA) Chinese American scientists Norden E. Huang proposed Empirical Mode Decomposition(EMD) method. This signal processing method is considered to be a major breakthrough relative to Fourier transform in recent years [8]. The EMD is a kind of analysis method based on the data

and has good adaptability. This kind of method has its advantages for nonlinear nonstationary signal processing. The most important thing is that EMD decomposition results Intrinsic Mode Function(IMF) have clear physical meaning. In a word the EMD has obvious advantages in processing of the nonlinear signal for machinery like as mechanical seal products [9].

### b.ii Intrinsic Mode Function

The EMD's role is to convert the original signal into IMF. The IMF need to satisfy two conditions:

(1)The number of extreme value point and the zero number should be equal or only differ by one.

$$(N_z - 1) \leq N_e \leq (N_z + 1) \quad (1)$$

(2)Local mean value of the up envelope defined by the maximum and the down envelope defined by the minimum should be equal to zero.

$$[f_{\max}(t) + f_{\min}(t)]/2 = 0 \quad (2)$$

### b.iii Empirical Mode Decomposition Process

EMD gradually dissociate IMF from the complex original signal, so EMD method also known as the sifting Process. The EMD decomposition process based on the following assumptions:① Signal at least have a maximum and a minimum;②Signal characteristics is determined by the distance between the extreme point; ③If lack of extreme point, signal data sequence still contains turning points. The extreme point can obtain through making derivative of the signal for one or many times. The decomposition result can be obtained by integrating the extreme points.

Based on the above assumptions, the specific shifting process is as follows:

(1)For a signal  $x(t)$ , first of all count all the extreme value point of it. Using the third-order spline interpolation obtain the original signal's up envelope and down envelope. Working out the average of the up envelope and down envelope, the result recorded as  $m(t)$ :

$$m(t) = [x_{\max}(t) - x_{\min}(t)]/2 \quad (3)$$

(2) $x(N)$  subtract  $m_1(N)$ , the results recorded as  $h_1(N)$ .

$$x(N) - m_1(N) = h_1(N) \quad (4)$$

(3)If the spline curve of  $h_1(N)$  meet the IMF two conditions, then

$$imf_1(N) = h_1(N) \quad (5)$$

If the spline curve of  $h_i(N)$  don't satisfy the *IMF* two conditions, then repeat the step(1) and step (2) until the spline curve of  $h_i(N)$  meet the *IMF* two conditions, and the abstracted result recorded as:

$$imf_1(N) = h_{ik}(N) \quad (6)$$

(4)  $imf_1(N)$  is separated from the sequence  $x(N)$ . The residual data  $r_1(N)$  is recorded as:

$$r_1(N) = x(N) - imf_1(N) \quad (7)$$

(5) If the average of the up and down envelope is a monotonic function or the average amplitude is less than the threshold, the process of decomposition should be end; If not,  $r_1(N)$  should be defined as original signal to repeat the above steps. The residual signal of the each process are written as

$$\begin{aligned} r_2(N) &= r_1(N) - imf_2(N) \\ &\vdots \\ r_n(N) &= r_{n-1}(N) - imf_n(N) \end{aligned} \quad (8)$$

Once  $r_n(N)$  was a monotonic function or its amplitude is less than the threshold, the loop should terminate.  $x(N)$  is given by the expression:

$$x(N) = \sum_{i=1}^n imf_i(N) + res(N) \quad (9)$$

The  $res(N)$  is residual function in the above Eq. It represents the signal average trend. The essence of the EMD method is that the decomposition processing is a shifting process. First separated the smaller time scales component from the original signal, then separated the bigger time scales component. So the EMD is considered a set of high-pass filter.

### c. Signal Processing

The eddy current signal is decomposed by EMD method into IMF component, each of IMF is shown in the Figure 4.

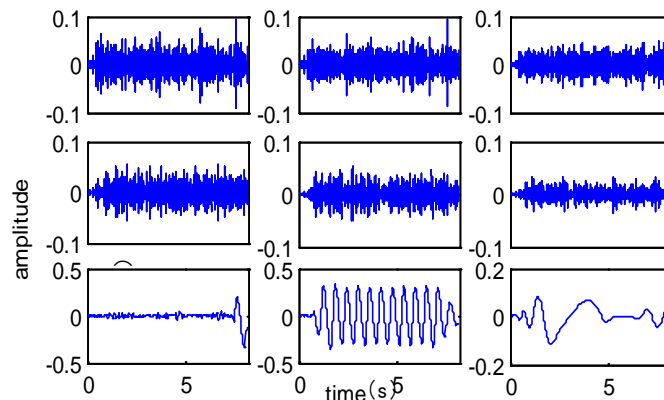


Figure 4. IMF components.

Each IMF components spectrum by FFT transformation is shown in Figure5. According to energy distribution characteristics of each component, the false components are eliminated by correlation coefficient filtering.

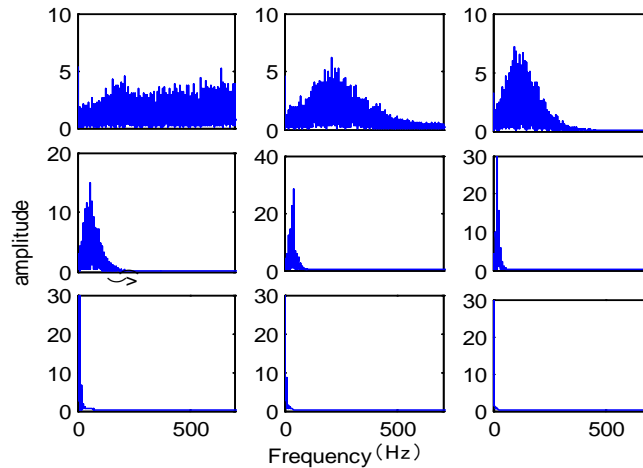


Figure 5. IMF components spectrum.

From the above figure we can obviously see that the energy of eddy current signal is mainly concentrated in the top six components. The first three components are almost noise. The following three components have the same frequency domain, which are mainly generated by vibration of fluid film. The last three components are sine wave parts. Refactoring the top six components(the first three component's amplitude is adjusted) to get the film thickness information. The refactoring eddy current signal is shown in the Figure 6.

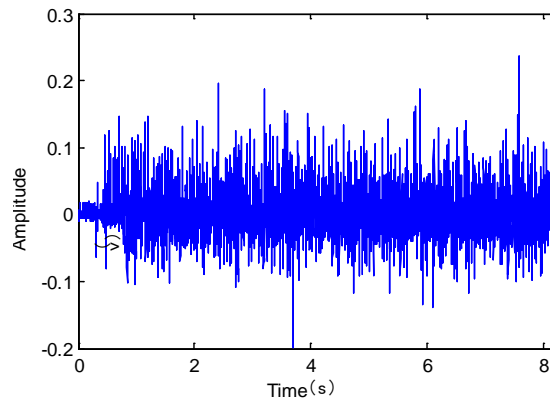


Figure 6. Eddy current signal.



Eliminating the abnormal value from the eddy current signal by 3-delta rule, the film thickness is obtained through converting the voltage signal to distance value. The actual thickness of the fluid film is respectively shown in Figure 7 at the medium presser of 0.5Mpa, 2Mpa, 5Mpa and 10Mpa. In each group, the spindle speed is changed from 0  $\text{r}\cdot\text{min}^{-1}$  to 1500  $\text{r}\cdot\text{min}^{-1}$ . It shows that the range of the film thickness is 8~23 $\mu\text{m}$ . The film thickness increases with the increasing of medium pressure. And the film thickness increased with the spindle speed varied from 0  $\text{r}\cdot\text{min}^{-1}$  to 300  $\text{r}\cdot\text{min}^{-1}$ , but decrease with the spindle speed varied from 300  $\text{r}\cdot\text{min}^{-1}$  to 1500  $\text{r}\cdot\text{min}^{-1}$ .

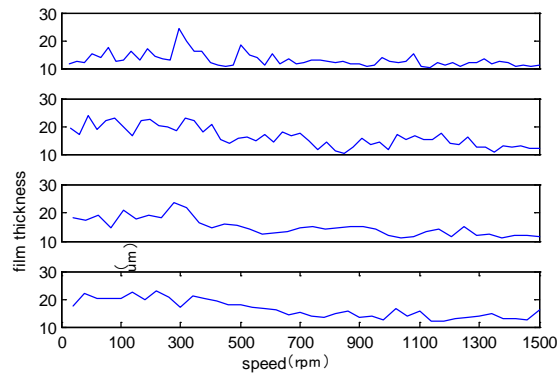


Figure 7. Curves of film thickness at variable speed.

Similarly, the film thickness curves with variable pressure at constant spindle speed are shown in Figure 8. The curves observed in Figure 8 are the actual thickness of the fluid film respectively at the spindle speed of 100, 300, 500, 700, 900, 1100, 1300, and 1500  $\text{r}\cdot\text{min}^{-1}$ , with the water pressure changed from 0.5MPa to 10MPa.

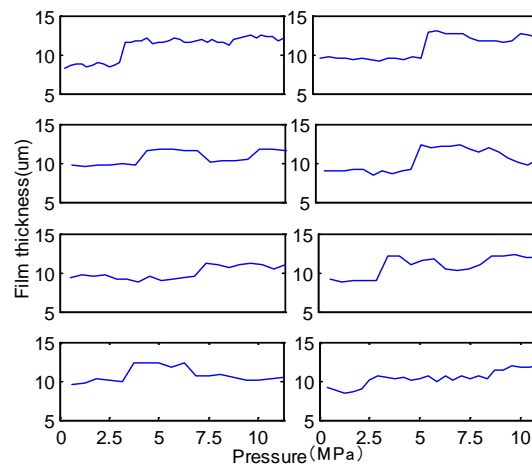


Figure 8. Curves of film thickness with variable pressure.

It is obvious that the film thickness increases with the increasing of medium pressure. It shows that the range of the film thickness also is 8~23um.

Based on the above information, the film thickness can be divided into 4 patterns as thin, medium, thick and above normal, as TABLE 2 shows.

Table 2: Patterns of film thickness

Patterns	Thickness
Thin	<8um
Median	8~15um
Thick	15~23um
Above normal	>23um

### III. INDIRECT MEASUREMENT

#### a. Monitoring Experiments

##### a.i Apparatus

An AE sensor is utilized to measure the friction between the two seal rings. It is fixed on the lateral of stationary ring by magnetic adsorption, as Figure 9 shows.

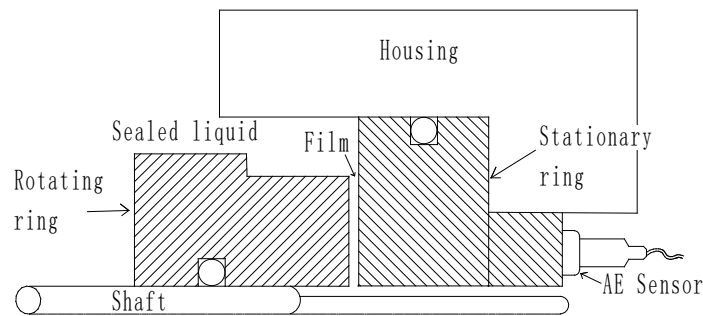


Figure 9. Curves of film thickness with variable speed.

AE sensor main parameters are given as below.

Type: Kistler8152B12SP; Range:50-400KHz; Sensitivity:57V/( m·s-1); Sampling frequency: 2MHz.

### a.ii Experiment Data

The wave of AE signal and its FFT spectrum are respectively shown in Figure 11 and Figure 12. The signal is obtained at the spindle speed of  $500 \text{ r}\cdot\text{min}^{-1}$ . The thickness of the fluid film can't be measured by AE signal directly. Little information about film thickness can be got directly from it. However, AE signal contains abundant information about the friction of mechanical seal end faces. And it is firmly related to the film thickness. First, AE signal features are extracted by wavelet packet, and optimized by kernel principal component analysis(KPCA). Then, a recognition model based on two-level BP ANN is built. Finally, the film thickness can be recognized by the artificial intelligent recognition system.

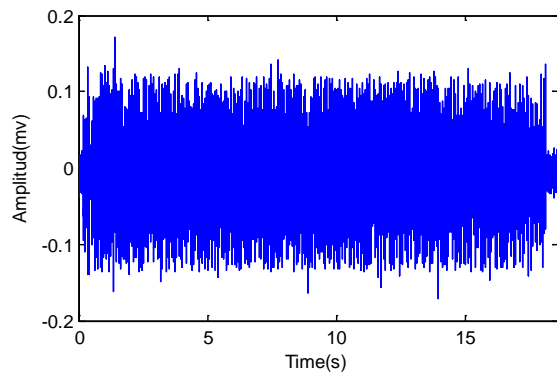


Figure 10. Curves of AE signal.

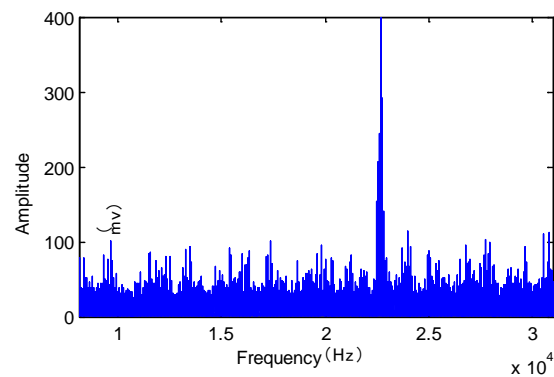


Figure 11. AE signal's spectrum.

### b. Method

Since AE sensor is very sensitive to any information including noise, which usually cause strong disturbance. The better features are difficult to be extracted. KPCA is used to optimize AE signal's features. Original feature dimension and nonlinearity all can be reduced by this method.

#### b.i KPCA Theory

As a classical approach for linear dimension reduction, principal component analysis (PCA) is always used to exact the principal component from multi-dimensional variables [10]. However, some useful information of the features may be broken by PCA, because more useful nonlinear correlation is sharply eliminated.

KPCA is an improved approach based on PCA for nonlinear dimension reduction [11]. Through projecting signal sample  $x$  from  $n$  to  $N$  ( $N > n$ ) dimensional space by an unknown mapping  $\phi$ , KPCA makes a new function  $\phi(x)$  linearly separable in the  $N$  dimensional space. The kernel function  $K\langle x_i, x_j \rangle$  is always used as the unknown mapping  $\phi$ .

Here,  $x_i, x_j$  is the  $i$ -th and  $j$ -th component vector ( $x$  is an  $m \times n$  matrix). The covariance matrix of the high dimension vector  $\phi(x_j)$  is given by:

$$\bar{C} = \frac{1}{m} \sum_{j=1}^m \phi(x_j) \phi(x_j)^T \quad (10)$$

Inferred from  $\lambda v = \bar{C} v$ :

$$v = \sum_{j=1}^m \frac{\phi(x_j)^T v}{\lambda m} \phi(x_j) \quad (11)$$

Where  $\lambda$  is eigenvalue of  $\bar{C}$ , and  $v$  is its eigenvector. So  $v$  is linear correlation about  $\phi(x_j)$ .

$$v = \sum_{j=1}^m \alpha_j \phi(x_j) \quad (12)$$

The kernel function  $K\langle x_i, x_j \rangle = \phi(x_i)^T \phi(x_j)$  is defined as the position of  $(i, j)$  in  $K$ , so:

$$m \lambda \alpha = K \alpha \quad (13)$$

Where  $\alpha = (\alpha_1, \dots, \alpha_m)^T$ . A formula  $\alpha^T \alpha = 1/m \lambda$  is used for normalization of  $v$ . To a test sample  $v$ , the projection on the direction of  $v$  is given as follows:

$$\phi(x_l)^T v = \sum_{i=1}^m \alpha_i K \langle x_l, x_i \rangle \quad (14)$$

Any symmetric function satisfied Mercer condition can be used as the kernel function[12]. Generally, the mean of  $\phi$  is proposed as 0, thus  $K$  must be normalized. KPCA processing is given as following:

- (1) Set up kernel function matrix  $K$  based on radial basis function.
- (2) Obtain eigenvalue  $\lambda$  and vector  $\alpha$  by function 13, and sort  $\lambda$  as  $\lambda_1 > \lambda_2 > \dots > \lambda_m$ .
- (3) Choose  $\lambda_1$  to  $\lambda_p$  ( $p < n$ ) as the principle elements, if the sum of them is more than 95% of all. Their corresponding eigenvector  $\alpha$ , is used as the direction where the kernel function projects on.
- (4) To any data sample, a new  $p$ -dimensional vector features can be obtained through projecting them on those  $p$  directions.

### b.ii Cascaded ANN Recognition

Artificial neural network (ANN) is a self-adaptable, nonlinear signal processing system based on the cross correlation of large numbers of artificial neurons [13, 14]. Since ANN has good classifying ability and self-learning system, it is widely used in the field of fault diagnosis, condition monitoring and image recognition etc. Back propagation (BP) ANN is a one of the earliest ANN model. The process of BP is made of signal forward propagation and error backward propagation [15]. A typical topology of three-layer BP ANN is shown in Figure 12.

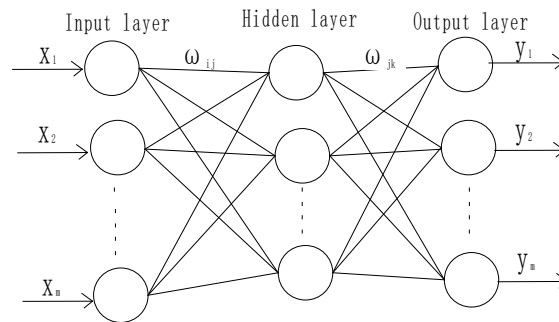


Figure 12. Topology of three-layer BP ANN.

As the input of BP ANN,  $(x_1, x_2, \dots, x_n)^T$  is the features of AE signal.  $(y_1, y_2, \dots, y_m)^T$  is the output.  $\omega_{ij}$  and  $\omega_{jk}$  stand for connected weights. While a feature vector is input, a recognition can be get from the output.

Multi-level ANN refers to which has two or more levels of network. The output of the former level is the input of the later. The second level ANN recognition can be achieved based on the results of the first recognition, and the final output fuses the results of the all former.

A cascaded decision recognition model based on multi-neural network is presented, and it has higher recognition rate than single ANN [16]. A two-level ANN with four patterns is shown in Figure 13. The four patterns is named as  $D_1$ ,  $D_2$ ,  $D_3$  and  $D_4$ , which are four continuous or nearby data segments. Because disturbed by noise, the results got by the first recognition via  $BP_1$  may have four kinds.

- (1) The four recognitions are the same.
- (2) Two of the four recognitions are the same.
- (3) Three of the four recognitions are the same.

(4) Every recognition is different from each other.

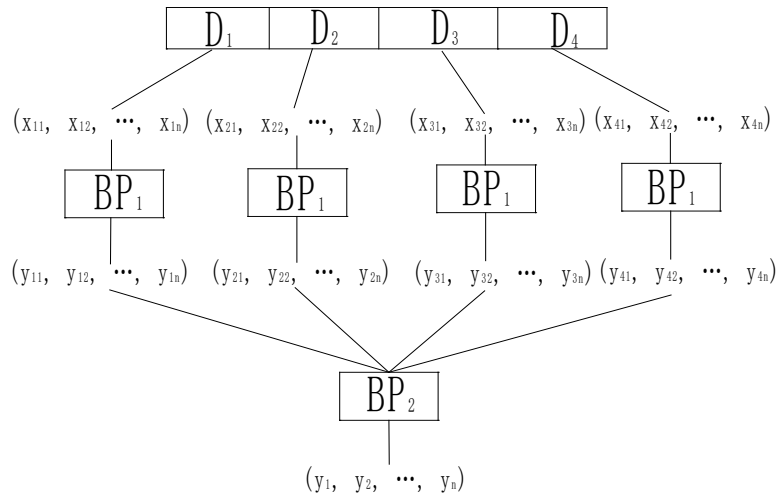


Figure 13. Topology of a double-level ANN.

There may have four results. This is a new question about fuzzy clustering. However it can be solved by another ANN. The second ANN BP<sub>2</sub> fuses the four output of BP<sub>1</sub>. Its output is the final decision.

### c. Feature extraction

According to TABLE 2, 48 film thickness patterns are evenly extracted by the difference of medium pressure and spindle speed. Each pattern contains 3 million continuously collected points, which are divided into equal 4 data segments. Thus there are 192 data segments in each pattern.

Every data segment is decomposed into 8 components by 'db1' wavelet packet. The components c1 to c8 are shown in Figure 14.

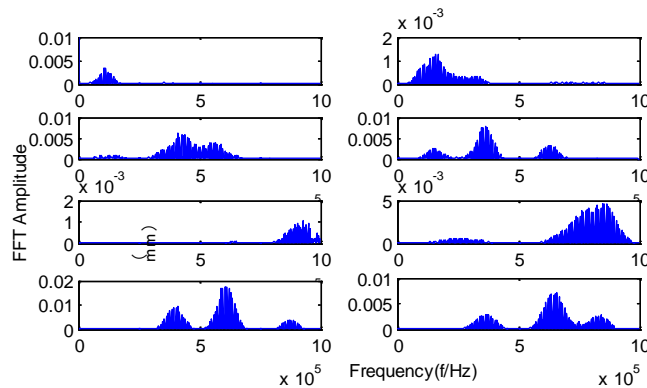


Figure 14. Decomposed signal by wavelet packet.

Since the statistical regularities of the information about the film thickness are unknown, features should be extracted as many as possible. Thus eleven features are extracted to each component in frequency domain. The formulas of them are defined as follows.

Root mean square: Reflect the whole power of signal.

$$RMS = \sqrt{\frac{1}{n} \sum_{i=1}^n x_i^2} \quad (15)$$

Peak factor: Reflect the signal strength.

$$C_f = \frac{x_{peak}}{\sqrt{\frac{1}{n} \sum_{i=1}^n x_i^2}} \quad (16)$$

Variance: description of disperse degree of stochastic process around the mean value.

$$\sigma_x^2 = \sum_{i=1}^N (x_i - \bar{X})^2 \quad (17)$$

Kurtosis coefficient: Reflect the large amplitude pulse in signal.

$$K_v = \frac{\frac{1}{n} \sum_{i=1}^n (x_i - \bar{x})^4}{\left(\frac{1}{n} \sum_{i=1}^n x_i^2\right)^2} \quad (18)$$

Margin coefficient: Reflect the anti-interference capacity of signal.

$$CL_f = \frac{x_{\max}}{\left(\frac{1}{n} \sum_{i=1}^n \sqrt{|x_i|}\right)^2} \quad (19)$$

Asymmetry index: Reflect the asymmetry degree of signal.

$$\beta = \frac{\frac{1}{n} \sum_{i=1}^n (|x_i| - \bar{x})^3}{\frac{1}{n} \sum_{i=1}^n (x_i)^3} \quad (20)$$

Frequency centre of gravity: Reflect the change of the gravity frequency centre of signal.

$$f_c = \frac{\sum_{i=1}^n f_i p_i}{\sum_{i=1}^n p_i} \quad (21)$$

Frequency variance: Reflect the deviation between frequency and its centre.

$$vf = \frac{\sum_{i=1}^n (f_i - f_c)^2 p_i}{\sum_{i=1}^n p_i} \quad (22)$$

Frequency mean square: Reflect the spectral energy of signal.

$$msf = \frac{\sum_{i=1}^n f_i^2 p_i}{\sum_{i=1}^n p_i} \quad (23)$$

Wavelet energy proportion: Reflect the energy proportion between the decomposed components and original signal.

$$pro = \frac{\sum_{i=1}^n x_i^2}{Pow(X)} \quad (24)$$

Wavelet signal entropy: Reflect the amount of information of each component.

$$H = \sum_{i=1}^n P_i \log P_i \quad (25)$$

In the above formula (15) ~ (25),  $x_i$  is the  $i$ -th sampling point;  $x_{peak}$  is signal peak;  $p_i$  is FFT amplitude on  $f_i$ ;  $Pow(X)$  is the energy of original signal;  $P_i$  is the probability of  $x=x_i$ . There are 88 features obtained in each one data segment. In such number of features, there must be have much redundant information among them. So it need dimension reduction. KPCA is used to exact the principal component from multi-dimensional variables. Feature vectors are orthogonally transformed in high dimension space and its principal components are extracted. The number of the features reduces from 88 to 13 through KPCA.

#### d. Cascaded Decision

The cascaded decision frame has two level networks. The first level is built by BP1. The inputs are those features which are reduced by KPCA, outputs are the primary decision. In each pattern, 24 set dates are chosen as training samples of BP1, and the other 24 sets are testing samples. The recognition rate of BP1 is shown as in Figure 15. It is obviously that the recognition rate of BP1 is not good, and it strictly decreases with increasing of the film thickness.



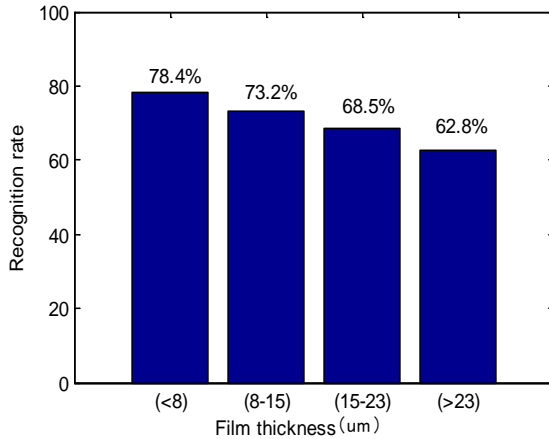


Figure 15. Recognition rate of BP1.

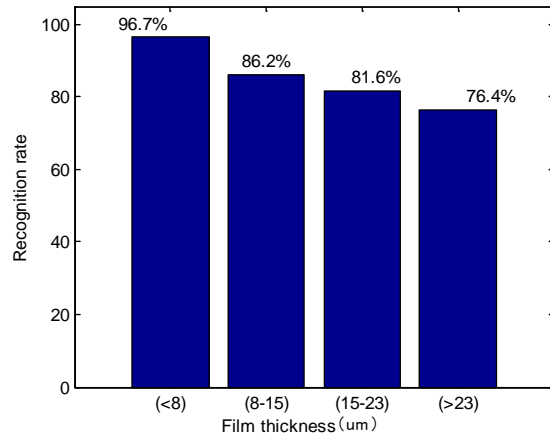


Figure 16. Recognition rate of BP2.

In order to resolve the above question, the second level network BP2 is built to improve the recognition effect. First sort the four outputs of each pattern according to their max confidence values in descending order. For instance, if the four outputs are given as (0.540, 0.153, 0.027, 0.280) (0.231, 0.243, 0.033, 0.495) (0.142, 0.098, 0.721, 0.039), (0.340, 0.273, 0.127, 0.260), their max confidence values are 0.540, 0.495, 0.721, 0.340. Then they should be sorted the order as (0.142, 0.098, 0.721, 0.039) (0.540, 0.153, 0.027, 0.280) (0.231, 0.243, 0.033, 0.495) (0.340, 0.273, 0.127, 0.260), which is a new output vector. The new output vectors are used as the input of next level BP2. The recognition rate of BP2 is shown in Figure 16.

Compared with Figure 15 and Figure16, it is obvious that cascaded decision has higher recognition rate than single ANN, and nice recognitions can be obtained as the film thickness is thinner than 8um.

## VI. CONCLUSIONS

In order to measure the film thickness of mechanical seal, AE and eddy current sensors have been used in this study. Using eddy current sensors realized direct measurement, and using AE sensor realized recognition of the film thickness indirectly. In a word, it is realized the transformation of film thickness measurement from inner side directly measure to external indirectly measure. Some conclusions can be get as follows.

- (1) The film thickness is accurately measured by eddy current sensor. It increases with the seal chamber pressure increases. However it first increases with the spindle speed, and then decreases when the spindle speed over 300 r•min<sup>-1</sup>.
- (2) AE signal features have been extracted by wavelet packet, optimized by KPCA which is used to reduce feature dimension without incurring excessive information loss. Through cascaded recognition network, the recognition rate is higher than single level .
- (3) This method also can be applied to diagnose the failure of mechanical seals and makes the prediction of the failure of mechanical seals possible.

### ACKNOWLEDGEMENTS

This work is supported by the National major project of science and technology achievement transformation: Nuclear power plant important pumps mechanical seal achievements transformation.

### REFERENCES

- [1].Sun Jianjun, Wei Long, Gu Boqing. The Development Course and The Research Trend of Mechanical Seal. Lubrication Engineering, Lubrication Engineering, Vol.4, 2004, pp.128-134.
- [2] G. Astridge and M. D. Longfield. Capacitance measurement and oil film thickness in a large-radius disc and ring machine, Vol.182, No.14, 1967, pp.89-96.
- [3] P. C. Chu and A. Cameron. Flow of electric current through lubricated contacts. ASLE Transactions, Vol.10, No.3, 1967, pp.226-234.
- [4] Etsion,I. Experimental of the dynamic behavior of non-contacting coned-face mechanical seals. ASLE Transactions, Vol.27, No.3, 1984, pp.263-270.
- [5] W. B. Anderson, J. Jarzynski and R. F. Salant. A condition monitor for liquid lubricated mechanical seals. Tribology Transactions, Vol.44, No.3, 2001, pp.479-483.
- [6] T. Reddyhoff, R.S. Dwyer-Joyce, and P. A new approach for the measurement of film thickness in liquid face seals. Tribology Transactions, Vol.51, No.2, 2008, pp.140-149.
- [7] J. Miettinen and V. Siekkinen. Acoustic emission in monitoring sliding contact behaviour. Wear, Vol.183, No.2, 1995, pp.897-900.

- [8].Cai Yanping, Li Aihua, Wang Tao,et al. Based on The EMD - Wigner Ville - internal Combustion Engine Vibration Time-frequency Analysis. *Journal of Vibration Engineering*, Vol.10, No.4, 2010, pp.430-437.
- [9].Xu Dong. Ball Bearing Fatigue Residual Life Analysis and The Forecast Method Research. Wuhan, Doctor of Engineering thesis, National University of Defense Technology, China, 2011, pp.205.
- [10] Shaojiang Dong and Tianhong Lou. Bearing degradation process prediction based on the PCA and optimized LS-SVM model. *Measurement*, Vol.46, No.9, 2013. pp.3143-3152.
- [11] K.I. Kim, S. H. Park, and H. J. Kim. Kernel principal component analysis for texture classification. *IEEE Signal Processing Letters*, Vol.8, No.2, 2011, pp.39-41.
- [12] Weilin Li, Pan Fu, Weiqing Cao. Study on Feature Selection and Identification Method of Toll Wear States Based on SVM. *International Journal on Smart Sensing and Intelligent Systems*, Vol.6, No.2, 2013, pp.448-465.
- [13] S.C.Mukhopadhyay, Novel Planar Electromagnetic Sensors: Modeling and Performance Evaluation, *Sensors* 2005, 5, 546-579, ISSN 1424-8220 © 2005 by MDPI <http://www.mdpi.org/sensors>, 2005.
- [14] G. S. Vijay, H.S. Kumar and N.S. Sriram et al. Evaluation of effectiveness of wavelet based denoising schemes using ANN and SVM for bearing condition classification. *Computational Intelligence and Neuroscience*, Vol.12, 2012, pp.46-51.
- [15] S.C.Mukhopadhyay, “A Novel Planar Mesh Type Micro-electromagnetic Sensor: Part I - Model Formulation”, *IEEE Sensors journal*, Vol. 4, No. 3, pp. 301-307, June 2004.
- [16] P. Sam Paul and A. S. Varadarajan. ANN assisted sensor fusion model to predict tool wear during hard turning with minimal fluid application. *IJMMM*, Vol.13. No.14, 2013, pp.398-413.
- [17] S.C.Mukhopadhyay, “A Novel Planar Mesh Type Micro-electromagnetic Sensor: Part II – Estimation of System Properties”, *IEEE Sensors journal*, Vol. 4, No. 3, pp. 308-312, June 2004.
- [18] Benny Karunakar and D. L. Datta. Prediction of defects in castings using back propagation neural networks. *IJMIC*, Vol.3, No.2, 2008, pp.140-147.
- [19] S.C.Mukhopadhyay, “Quality inspection of electroplated materials using planar type micro-magnetic sensors with post processing from neural network model”, *IEE Proceedings – Science, Measurement and Technology*, Vol. 149, No. 4, pp. 165-171, July 2002.

[20] Zhao Peng. Study on the vibration fault diagnosis method of centrifugal and system implementation. Doctor of Engineering thesis, North China Electric Power University(Beijing), China, 2011, P68.